

# physica **p** status **s** solidi **S**

[www.pss-journals.com](http://www.pss-journals.com)

**reprint**



# A study on linearity compensation of pressure-level sensor using contact-resistance change

Jung-Ho Park<sup>\*,1</sup>, Yun-Jin Jeong<sup>2</sup>, Dong-Won Yun<sup>1</sup>, So-Nam Yun<sup>1</sup>, Young-Bog Ham<sup>1</sup>, Dong-Weon Lee<sup>\*,2</sup>, and Dong-Hwan Lee<sup>3</sup>

<sup>1</sup> Korea Institute of Machinery and Materials, 156 Gajeongbuk-Ro, Yuseong-Gu, Daejeon 305-343, Republic of Korea

<sup>2</sup> Chonnam National University, 77 Yongbong-Ro, Buk-Gu, Gwangju 500-757, Republic of Korea

<sup>3</sup> Montrol Co. Ltd., 35 Techno 9-Ro, Yuseong-Gu, Daejeon 305-510, Republic of Korea

Received 24 November 2013, revised 13 June 2014, accepted 17 June 2014

Published online 17 July 2014

**Keywords** contact resistance, MEMS, pressure sensors

\* Corresponding authors: e-mail jhpark@kimm.re.kr; mems@jnu.ac.kr, Phone: +82 42 868 7607, Fax: +82 42 868 7335

In this study, a novel MEMS pressure-level sensor using contact-resistance change is presented. The resistance change results from a physical contact between a micropatterned switch array and a conductive diaphragm with an applied pressure. First, a concept and a working principle of the proposed pressure-level sensor are introduced and basic characteristics of the fabricated prototype sensor with serially connected resistors and electrodes are experimentally tested. Then, a new approach

for linearity compensation of the proposed mechanism is analytically investigated with contact analysis results obtained by using commercial FEM tools, which is to control a pattern slope of the deposited ITO resistor. Finally, based on the obtained analysis results, a pressure-level sensor is refabricated and experiments including durability test are performed and discussed.

© 2014 WILEY-VCH Verlag GmbH & Co. KGaA, Weinheim

**1 Introduction** With recent progress in microelectromechanical systems (MEMS) technologies based on surface-micromachining and bulk-micromachining, many pressure sensors such as piezoresistive and capacitive types have been reported and investigated for industrial applications [1–8]. However, most of these pressure sensors have a few limited applications because of low stress strength, offset drift with temperature change, and a complicated electric circuit to amplify a feeble signal, although they have some advantages such as linearity, sensitivity, and better accuracy.

As an application field of MEMS pressure sensors, pressure-level sensors that are employing piezoresistive-type pressure sensors or strain gauges are used to measure a liquid level in storage tanks or vessels [9–11]. Then, a level sensor using plastic optical fibers was investigated because of the low cost and high flexibility and so on [12]. In general, the pressure-sensing method has been used for measurement of liquid level in industries instead of electrical methods due to the characteristics of a certain harmful liquid and its process conditions [9]. Those sensors need some amplifiers due to

the very weak electric signals and relatively complicated electric circuits for noise or temperature compensation.

Therefore, to overcome those disadvantages, a novel pressure-level sensor using the resistance change of a micropatterned switch array resulted from a physical contact of diaphragm with an applied pressure has been proposed and experimentally investigated [13–15]. In this study, to compensate the nonlinearity characteristic, a novel design method to control a pattern slope of the deposited resistor on Pyrex glass is attempted and basic characteristics of the refabricated sensor are experimentally investigated.

## 2 Design and fabrication of prototype sensor

**2.1 Concept and working principle** Figure 1a and b shows a concept and a working principle of the proposed pressure-level sensor using contact-resistance change [15–17]. It basically consists of a silicon substrate that has a thin-metal deposited diaphragm and a switch array micropatterned on Pyrex glass. The switch array to measure the pressure change is formed by connecting serially a few electrodes and resistances on a resistor made by indium tin oxide (ITO).

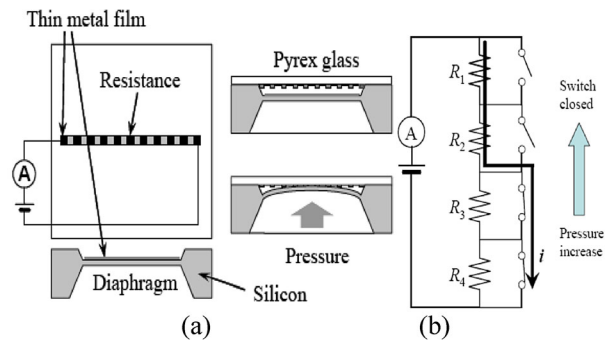


**Figure 1** (a) Concept and (b) working principle of the proposed pressure-level sensor using contact-resistance change.

The change of the electrical resistance between both ends of the ITO resistor is measured by using a simple electric circuit. When a pressure is applied to the diaphragm, the diaphragm is expanded to the glass and an initial contact between the diaphragm and the micropatterned pressure switch array is generated. Then, a change of contact resistance occurs with an applied higher pressure and it is converted to a sensor signal through an electric circuit. Here, there is a dead zone of pressure till the initial contact due to the mechanism. The switching electrode formed on the ITO resistor has a constant gap distance of about 100  $\mu\text{m}$ .

**2.2 Fabrication and basic characteristics** As shown in Fig. 1a, the designed pressure-level sensor is composed of two parts of silicon and glass. Figure 2a–d shows photographs of the fabricated silicon part, the glass part, the magnified switch array, and prototype sensor, respectively. Au electrodes with a 100- $\mu\text{m}$  gap distance are formed on the ITO resistor. A thin silicon diaphragm can be fabricated using a wet etching process. Here, the diaphragm thickness is 35  $\mu\text{m}$  and the gap distance between the

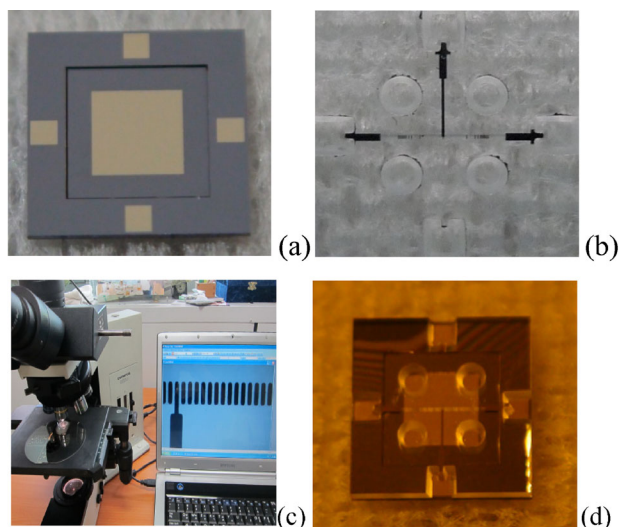


**Figure 2** Photographs of the fabricated prototype sensor: (a) silicon part, (b) glass part, (c) switch array, and (d) prototype sensor.

diaphragm and the glass is 30  $\mu\text{m}$ . The fabrication process starts with a silicon substrate (n-type, (100)) with a surface area of  $6 \times 6 \text{ mm}^2$  and a thickness of 0.3 mm. The silicon substrate is etched up to depth of 30  $\mu\text{m}$  in tetramethyl ammonium hydroxide (TMAH) 15% solution. Thin Au/Cr with a thickness of 0.21  $\mu\text{m}$  is then deposited by RF sputtering and lift-off is performed. Then, silicon backside etching is also performed. On the other hand, ITO patterning on Pyrex glass is performed and metal lift-off is also performed. Here, the distance between the Au/Cr electrodes formed on the ITO resistor could be adjusted for linearity compensation of sensor output. Holes through the glass are fabricated by a sand-blasting process for the ventilation of chamber between silicon and glass parts. The diameter of the hole is about 1.0 mm and the thickness of the glass part is not changed after the process. Finally, the glass is anodically bonded to the silicon substrate after a sanding process. The basic characteristic between the applied pressure and the resistance change is investigated using a simple experimental setup. A constant voltage is applied to both ends of the ITO resistor and the current change that is caused by the increase in the contact electrodes is measured with the source meter.

As the pressure increases, the resistance change caused by a diaphragm contact is generated and a value of resistance is gradually decreased. However, the result shows some problems such as insufficient linearity and a low pressure characteristic [14, 16].

### 3 Analysis and refabrication for linearization

**3.1 Contact analysis** Based on shape parameters of sensor chip and maximum stress with a pressure of 10 bar, a thickness of silicon diaphragm is changed to be 50  $\mu\text{m}$ . First of all, contact analysis is performed with different gap distance between diaphragm and bottom surface of Pyrex glass. The finite element analysis using the commercially available software, SAMCEF, is employed to expect the mechanical deflection of the conductive diaphragm as a function of applied pressure. The isotropic properties of the material are used in the simulation process because the analysis results with isotropic two-dimensional modeling are very close to those of the anisotropic three-dimensional modeling. For the FEM analysis, a Young's modulus of 169 GPa, a Poisson's ratio of 0.25, and a density of  $2330 \text{ kg m}^{-3}$  are used. The silicon substrate was modeled to a depth of 25–50  $\mu\text{m}$  from the top, and the diaphragm thickness was 50  $\mu\text{m}$ .

Figure 3 shows the obtained results of contact length with applied pressure. Nonlinearity could be confirmed due to the contact mechanism. According to the analysis results, the diaphragm started to contact with the ITO resistor at  $\sim 1.5$  bar. Considering the ease of the fabrication process, a gap distance of 30  $\mu\text{m}$  is selected in this study. Figure 4a and b shows the analysis results of diaphragm displacement and stress with a pressure of 10 bar. The highest stress is observed near the edges of the silicon diaphragm. It is also ascertained that the contact length is 1.53 mm and the



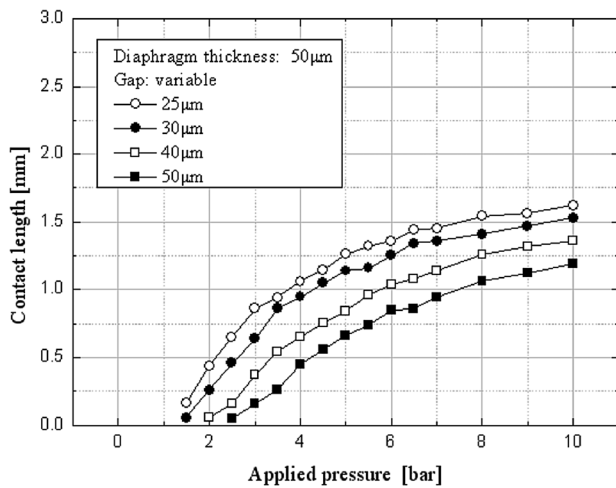


**Figure 3** Analysis results of contact length with different gaps.

maximum stress is 526 MPa with a diaphragm thickness of 50  $\mu\text{m}$  and a gap distance of 30  $\mu\text{m}$ .

**3.2 Linearization algorithm** To compensate a non-linearity of contact length with an applied pressure, it is required that a pattern slope of the deposited ITO resistor should be properly controlled, as shown in Fig. 5. The differential resistance  $\Delta R$  at an arbitrary distance of  $x$  from the center of diaphragm is derived as follows:

$$\Delta R = \rho \frac{\Delta x}{2t' \times h(x)}, \quad (1)$$

where  $t'$  and  $\rho$  are thickness of resistor and specific resistance, respectively. If the resistance changes with applied pressure, their ratio is constant for linearization, which is written as follows:

$$\frac{dR}{dP} = c. \quad (2)$$

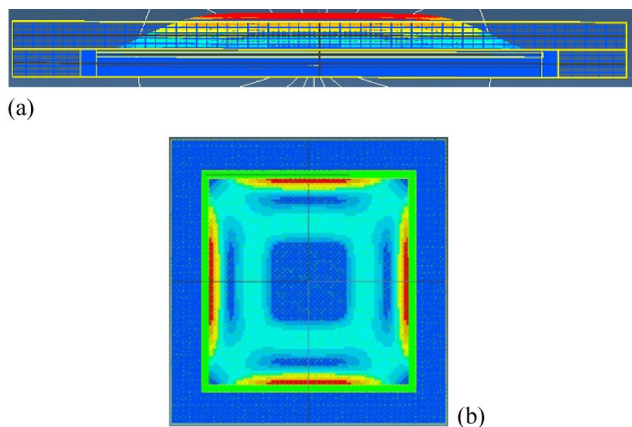


**Figure 4** Displacement and stress characteristics obtained by contact analysis with applied pressure of 10 bar: (a) diaphragm displacement profile and (b) stress characteristic.

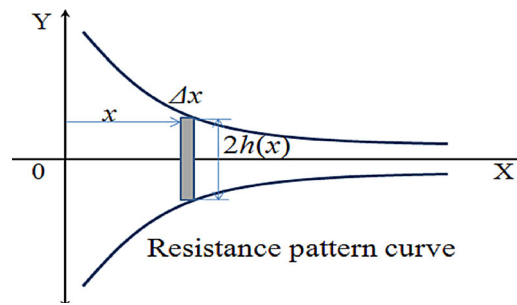


**Figure 5** Model of resistance pattern for linearization.

Considering  $x = f(P)$  and the chain rule, Eqs. (3) and (4) are derived as follows:

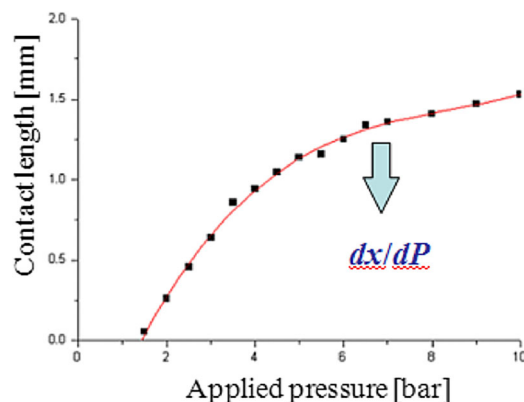
$$\frac{dR}{dP} = \frac{dR}{dx} \frac{dx}{dP}, \quad (3)$$

$$\frac{\rho}{2t' \times h(x)} \frac{dx}{dP} = c. \quad (4)$$

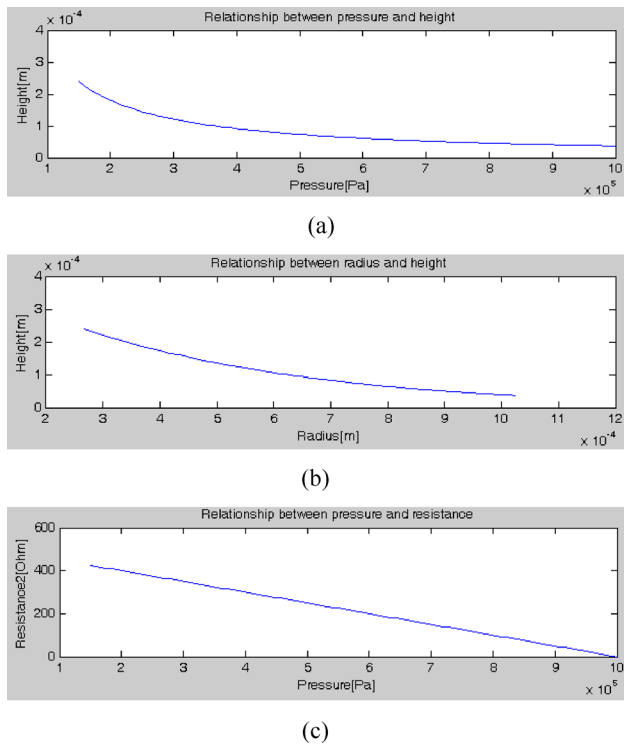
As shown in Fig. 6, if we derive  $dx/dP$  through curve fitting from the result of Fig. 3, a resistance pattern slope  $h(x)$  for compensation of linearity could be obtained.

Figure 7 shows a sample of the analysis results. Here,  $t' = 100 \text{ nm}$ ,  $\rho = 92 \times 10^{-4} \Omega \text{ cm}$  and  $c = 5000$ . The upper figure presents a pattern shape with applied pressure. The next figure is a pattern shape with the  $x$ -axis coordinate transformed from the applied pressure. The bottom figure indicates the resistance change with applied pressure. Figure 8 shows a resistance pattern from the center of the diaphragm for the fabrication process, which is equivalent to the first quadrant of ITO pattern on Pyrex glass.

**3.3 Refabrication and experiments** Figure 9a–c shows a schematic of an improved design, a photograph of a refabricated ITO pattern, and a pressure-level sensor, respectively. By using the refabricated sensor, the basic



**Figure 6** Curve fitting for linearization.



**Figure 7** Analysis results for linearization: (a) relation between pattern shape and pressure, (b) relation between pattern shape and x-axis coordinate, and (c) relation between resistance and pressure.

characteristics between applied pressure and measured resistance are experimentally investigated.

The obtained results are shown in Fig. 10. We can confirm that a dead zone of pressure is generated due to the contact mechanism. This means that this type of pressure sensor could be utilized only in the pressure range between contact and setting pressures. Also, it could be confirmed that a better linearization characteristic is achieved up to the pressure of 10 bar than the previous prototype [14]. Linearity in pressure ranges excluding a dead zone of pressure, is derived as 17% from 2 to 10 bar. Then, an experiment for repeatability and hysteresis is also done as shown in Fig. 11. From the obtained results between applied pressure and

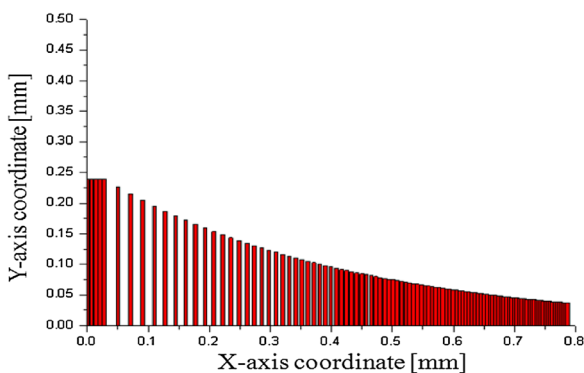


**Figure 8** Resistance pattern for fabrication process.

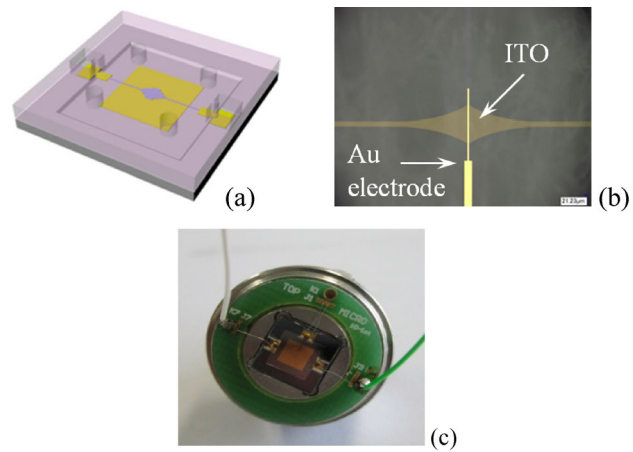


**Figure 9** Refabricated pressure-level sensor: (a) schematic of improved design, (b) ITO pattern, and (c) refabricated sensor chip.

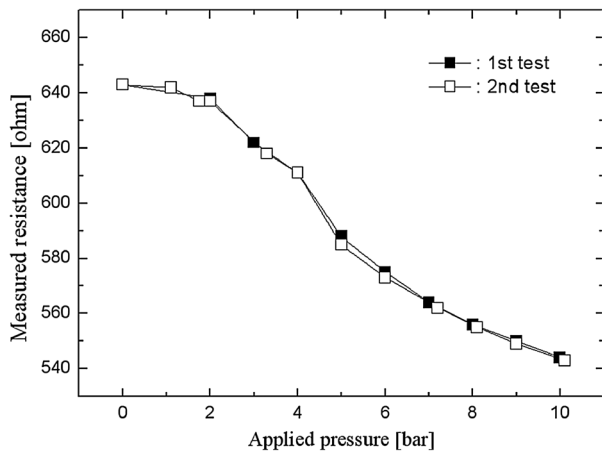


**Figure 10** Experimental results of the refabricated sensor.

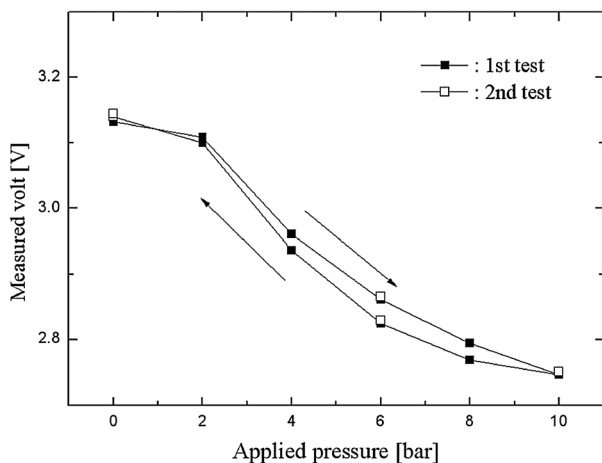


**Figure 11** Experimental results of the refabricated sensor.

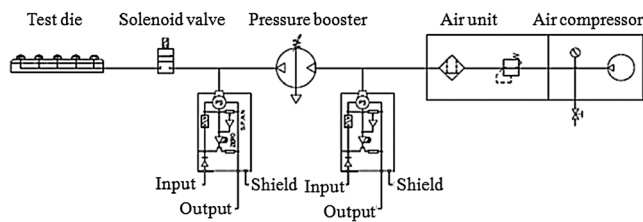


**Figure 12** Schematic of experimental apparatus for durability.

measured voltage, a repeatability of 2.9% and a hysteresis of 3.24% are calculated, respectively. The total accuracy of the fabricated pressure sensor is derived as 17.5%.

Although the accuracy is not as good as the other precision sensors, it is expected that calibration by data mapping and its application to a cost-effective level sensor can make up for the insufficient performance. Figure 12 shows a schematic of an experimental apparatus for a durability test. In general, it is difficult to increase a line pressure up to 10 bar in a pneumatic system with only a compressor. Therefore, a pressure booster was used for the durability test in this study. Photographs of each element of the constructed experimental apparatus are shown in Fig. 13a–d. The durability test is performed with applied pressures of 5 and 10 bar, respectively. The results are shown in Fig. 14. In experiments, sinusoidal waveforms of 5 and 10 bar are applied to the sensor up to the  $10^5$  times at 1 Hz. The resistance error of the total accuracy after the test is no more than 4%. The cause of error is the change of ITO resistance due to the temperature fluctuation. From the above experiments, the validity of the proposed pressure-level sensor should be verified, although the sensitivity needs some improvements.

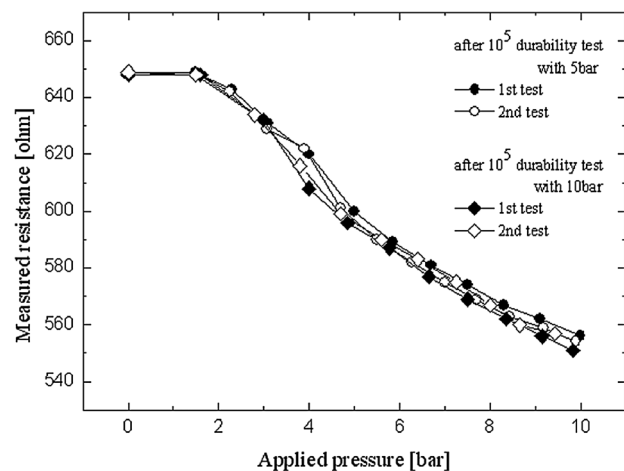


**Figure 14** Experimental results of durability test.

**4 Conclusions** In this study, a novel MEMS pressure-level sensor using resistance change resulted from a physical contact of diaphragm with an applied pressure was presented. For an improvement of nonlinearity of the fabricated prototype, an analytical study to control a pattern slope of the deposited ITO resistor on Pyrex glass was performed. Refabrication was also done and the basic characteristics including durability were experimentally investigated. From the results, we could confirm that the validity of the proposed pressure-level sensor is effective, although the sensitivity needs some improvements.

**Acknowledgements** This work was supported by the Technology Innovation Program (Innovation Cluster Program) through the Korea Innovation Cluster Foundation funded by the Ministry of Trade, Industry and Energy (MOTIE, Korea) (No. 1415119538).

## References

- [1] W. P. Eaton and J. H. Smith, *Smart Mater. Struct.* **6**, 530–539 (1997).
- [2] W. P. Eaton, J. H. Smith, D. J. Monk, G. O'Brien, and T. F. Miller, *Proc. SPIE* **3514**, 431–438 (1998).
- [3] D. S. Eddy and D. R. Sparks, *Proc. IEEE* **86**, 1747–1755 (1998).
- [4] S. Renard, *J. Micromech. Microeng.* **10**, 245–249 (2000).
- [5] C. Pramanik, H. Saha, and U. Gangopadhyay, *J. Micromech. Microeng.* **16**, 2060–2066 (2006).
- [6] W. H. Ko and Q. Wang, *Sens. Actuators A* **75**, 242–251 (1999).
- [7] O. Akar, T. Akin, and K. Najafi, *Sens. Actuators A* **95**, 29–38 (2001).
- [8] A. Huang, J. Lew, Y. Xu, Y.-C. Tai, and C.-M. Ho, *IEEE Sens. J.* **4**, 494–502 (2004).
- [9] T. M. Sarath, H. J. P. Subha, and F. Daniel, *Int. J. Adv. Res. Comput. Sci. Softw. Eng.* **3**, 118–121 (2013).
- [10] J. C. Hamelain, Freescale Semiconductor Inc., Application Note AN1516, Rev 4, 5 (2005).
- [11] A. Le, Literature No. SNAA127, [signalpath.national.com/designer](http://signalpath.national.com/designer).

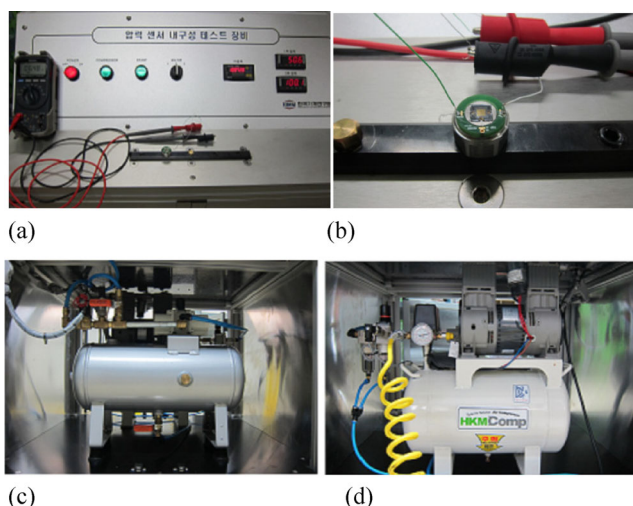


**Figure 13** Photographs of constructed experimental apparatus: (a) test die, (b) test sensor, (c) pressure booster, and (d) air unit with compressor

- [12] M. Foroni, M. Bottacini, F. Poli, A. Cucinotta, and S. Selleri, Proc. SPIE **6189**, 618927 (2006).
- [13] J.-H. Park, D.-W. Youn, D.-W. Lee, S.-Y. Ham, and J.-D. Jo, Proc. KSME Spring Conference (2006), pp. 3203–3207 (in Korean).
- [14] Y.-J. Jeong, J.-H. Park, Y.-J. Han, and D.-W. Lee, Proc. 15th Korean MEMS Conference (2013), pp. 161–162 (in Korean).
- [15] J.-H. Park, J.-Y. Won, S.-N. Yun, D.-W. Lee, and Y.-J. Han, Proc. KSME Spring Conference (PD Division) (2012), pp. 165–166 (in Korean).
- [16] C.-S. Park and D.-W. Lee, Rev. Sci. Instrum. **81**, 055103-1 (2010).
- [17] Y.-J. Jeong, J.-H. Park, and D.-W. Lee, Sens. Actuators A (2014) (under review).